Journal of Materials Science: Materials in Electronics (2018) 29:2949–2957
https://doi.org/10.1007/s10854-017-8225-3

Low temperature sintering and role of room-temperature phase transition in the electrical properties of $(Ba_{0.85}Ca_{0.15})(Zr_{0.10}Ti_{0.90})_{1-x}(Cu_{1/3}Nb_{2/3})_xO_3$ ceramics

Huaidang Zhao[1] · Weibing Ma[1] · Jingdong Guo[1] · Xiangrong Zang[1] · Peishuang Miao[1] · Minjie Ma[1] · Feiyang Zhang[1]

Received: 27 August 2017 / Accepted: 7 November 2017 / Published online: 18 November 2017

Abstract
Perovskite type $(Ba_{0.85}Ca_{0.15})(Zr_{0.10}Ti_{0.90})_{1-x}(Cu_{1/3}Nb_{2/3})_xO_3$ (x = 0.00, 0.005, 0.01, 0.015 and 0.02) (abbreviated as BCZT-1000xCN) lead-free ceramics were prepared via a conventional solid-state reaction method. The phase structure, microstructural morphology and electrical properties of BCZT-1000xCN ceramics with different CuO/Nb_2O_5 content were systematically investigated. The phase identifications of the ceramic samples were investigated by X-ray diffraction and the results indicated that all samples showed a pure perovskite phase with no secondary phase. Microstructure, electrical properties and polarization–electric field (P–E) hysteresis loops indicated that a small amount of CuO/Nb_2O_5 (x = 0.005–0.02) addition affected the properties obviously. The addition of CN effectively resulted in the decrease of grain sizes and slightly improved uniformity of grains in BCZT ceramics. Moreover, the results revealed that the addition of CN significantly improved the sinterability of BCZT ceramics which resulted in a reduction of sintering temperature from 1450 to 1400 °C without sacrificing the high piezoelectric properties. Achieving a polymorphic phase transition point at room temperature about 20 °C could improve the piezoelectric properties of BCZT-1000xCN ceramics. Main piezoelectric parameters of BCZT-1000xCN ceramics were optimized around x = 0.01 with a high piezoelectric coefficient (d_{33} = 550 pC/N), a planar electromechanical coefficient k_p of 50%, a remnant polarization (P_r = 12.6 μC/cm^2), a high dielectric constant (ε_{rmax} = 6056) and a low dissipation factor (tanδ = 1.55%) at 1 kHz, indicating promising applications for lead-free piezoelectric ceramics.

1 Introduction

In recent years, the study of piezoelectric ceramic materials had made significant progress. Piezoelectric ceramics were a kind of important functional materials which could convert electric energy from mechanical energy. At present, lead-based piezoelectric ceramics as the functional materials, represented by lead zirconate titanate were widely used for piezoelectric actuators, sensors and transducers due to their good thermal stability and excellent electrical properties [1–3]. However, PbO volatile produced more pollution to the environment and damaged to human body in the preparation process of lead-based piezoelectric ceramics. With the recent growing demand for global environmental protection, the restriction of the use of certain hazardous substances in electrical and electronic equipment (RoHS) directive banned the placing on the European Union market of new electrical and electronic equipment containing more than agreed levels of lead in 1 July 2006. Consequently, from the viewpoint of long-term development of the world, seeking lead-free or low-lead content materials with more environmentally friendly benefits and competitive properties to replace the traditional Pb-based ceramics had become one of the most significant works [4].

In the research of Pb-free piezoelectric ceramics, considerable attention had been recently given to $(K_{0.50}Na_{0.50})NbO_3$-, $BiFeO_3$- and $Bi_{0.50}Na0._{50}TiO_3$-based ceramics because of their environmental issues, high Curie temperature, and good piezoelectric properties [4–12]. Moreover, their inferior piezoelectric coefficients (d_{33} = 490–570 pC/N) could match those of part Pb-based piezoelectric ceramics [13–16]. However, there is still some gaps between Pb-free piezoelectric ceramics and the high d_{33} values of lead-based

✉ Weibing Ma
tju11305@126.com

[1] Key Laboratory for Advanced Ceramics and Machining Technology of Ministry of Education, School of Materials Science and Engineering, Tianjin University, Tianjin 300072, China

ceramics ($d_{33} \approx 590$ pC/N for PZT-5H). Meanwhile, low-density, low temperature stability and relatively lower piezoelectric properties hindered their practical applications. Therefore, it was urgent to seek a new lead-free material system with higher piezoelectric properties to replace lead-based ceramics.

Barium titanate ($BaTiO_3$) was the earliest known perovskite-type ferroelectric ceramics and had five kinds of phase structures at different temperatures, but its piezoelectric constant (d_{33}) was still poor [17]. In order to improve the piezoelectric and dielectric properties, modified $BaTiO_3$ ceramics had recently been demonstrated to create the morphotropic phase boundary (MPB) at room temperature by doping Ca and Zr. The study acquired a high d_{33}, superior to that of lead zirconate titanate materials [18]. Numerous researches had discovered that the excellent piezoelectric performance was attributed to a triple point morphotropic phase boundary state (MPB), a coexistence of tetragonal, orthorhombic, and cubic phases close to room temperature [18–21].

In addition, the formation of a polymorphic phase transition point at room temperature also resulted in the BCZT materials having excellent piezoelectric behavior [18]. The investigator had found that the tricritical point led to strong temperature dependence in $(Ba_{0.85}Ca_{0.15})(Zr_{0.10}Ti_{0.90})O_3$ (BCZT) ceramics was above room temperature (~ 315 K), thus a relatively low d_{33} value was achieved in this work. Therefore, it was important to decrease the polymorphic phase transition point down to room temperature for further improving the piezoelectric properties of these materials, which had become the main key research direction currently. In addition, lead-free BCZT based ceramics showing excellent piezoelectric properties (piezoelectric coefficient; $d_{33} \approx 600$ pC/N) and good dielectric properties were attributed to the use of high calcination (1300–1350 °C) and sintering temperature (1500–1550 °C) as well as very long dwelling times [18]. Recently, some authors also found that Ca and Zr codoped $BaTiO_3$ ceramics with a dense microstructure and a high d_{33} were obtained only by sintering in an industrial N_2 atmosphere as well as a high temperature [22]. For BCZT ceramics, the introduction of Zr into Ti site usually raised sintering temperature, and then the densification of ceramics became difficult [23]. However, BCZT ceramics could be well sintered at a lower temperature if a liquid-phase was formed during sintering process. It was well known that a small amount of suitable addition was an effective and simple method to modify electrical properties of piezoelectric ceramics. CuO was commonly chosen as a kind of sintering aid in lead-free ceramics to further improve piezoelectric properties and reduce the sintering temperature such as BNT-BZT, KNN and (Ba,Sr)(Ti,Zr)O_3 ceramics, because of its low melting point and formation of the liquid phase [24–26]. Meanwhile, Zheng et al. also found that CuO-modified Ba(Ti,Zr)O_3 ceramics had an excellent piezoelectric performance [27]. Furthermore, it was well known that the addition of Nb_2O_5 could slightly reduce the Curie temperature (T_c) of piezoelectric ceramics. We speculated on whether the additive of Nb_2O_5 could shift the tricritical point to room temperature and simultaneously caused a decrease in Curie temperature (T_c). The last but not least, the use of CuO/Nb_2O_5 as the additive could make the microstructure denser, resulting in an amelioration in the electrical properties and sintering temperature of piezoelectric ceramics [28–30].

Therefore, the purpose of this study was to present the effect of CN addition on the density, phase structure, electrical properties and sintering temperature of BCZT ceramics. The dielectric properties of BCZT-1000xCN ceramics were also measured as a function of temperature. A low sintering temperature and enhanced electrical properties of BCZT ceramics were obtained by the addition of CN, and the physical mechanism underlying some properties were also illustrated.

2 Experimental procedure

A conventional solid-state reaction technique was used to prepare $(Ba_{0.85}Ca_{0.15})(Zr_{0.10}Ti_{0.90})_{1-x}(Cu_{1/3}Nb_{2/3})_xO_3$ (x = 0.00, 0.005, 0.01, 0.015 and 0.02) (BCZT-1000xCN) lead-free piezoelectric ceramics. Reagent-grade powders, $BaCO_3$ (99.0%), $CaCO_3$ (99.0%), ZrO_2 (99.0%), TiO_2 (98.0%), CuO (99.0%) and Nb_2O_5 (99.9%) used as the raw materials were weighed and mixed in a centrifugal mill, as well as wet-homogenized with the addition of alcohol for 4 h and then dried. The dried mixtures were calcined at 1150 °C for 4 h. Thereafter, the mixtures were ball-milled in ethanol for 8 h, then dried, sifted and mixed with 7 wt % poly vinyl alcohol (PVA) solution. The mixed powder was pressed uniaxially into disk specimens with a diameter of 12 mm and a thickness of 1.2–1.5 mm under 100 MPa and consolidated by isostatic pressing at 200 MPa. After burning out PVA at 650 °C for 20 min to ensure that all the binder and organic materials were removed, the disks were sintered at 1400 °C for 4 h in a sealed alumina crucible.

The bulk densities of the sintered samples were measured by the Archimedes method and theoretical density of each composition was calculated from the XRD data. The phase identifications of the sintered samples were investigated by X-ray diffraction (XRD) (D/MAX-2500, Rigaku, Tokyo, Japan) using Cu Kα radiation with scanning at 8 °/min and 2θ range of 20–70°. Scanning electron microscopy (SEM, S4800, Hitachi, Japan) was used to observe the microstructure of the natural surface of the ceramics. The sintered samples were polished into disk samples and their thicknesses were from 0.8 to 1.0 mm. Silver electrodes were painted on the upper and bottom surfaces of the polished pellets, and

fired at 735 °C for 15 min for dielectric and piezoelectric characterization. After this, sintered samples were poled in silicone oil at room temperature under 5.0 kV/mm for 25 min. The relative dielectric constant and dielectric loss measurements were performed at room temperature with an LCR automatic meter(XC2810A, Tianjin Xin Ce Electronics Apparatus Technology Co., Ltd., Tianjin, China). The planar coupling K_p was determined by impedance analyzer(XFG-7, Shanghai YaMei Electric Appliance Co., Ltd. Shanghai., China). Planar electromechanical coupling factor k_p were calculated following IEEE standards. The temperature dependence of the dielectric constant and the dissipation factor of the specimen homogenously were measured with temperatures ranging from − 25 to 125 °C at a step of 1 °C/min. The piezoelectric constant d_{33} was measured by quasistatic d_{33} meter (ZJ-3AN, Institute of Acoustics Academic Sinica, Beijing, China) based on Berlincourt method. A standard ferroelectric tester(WS-2000, Tsinghua University, Beijing, China) was followed to measure the ferroelectric hysteresis P–E loops at a frequency of 1 kHz.

3 Results and discussion

The phase formation of the room temperature (T = 25 °C) BCZT-1000xCN lead-free piezoelectric ceramics were shown in Fig. 1a. From the XRD patterns, it could be seen that all samples exhibited pure perovskite phase (PDF#79-1482) with no secondary phase existing. To observe the phase evolution clearly, further observation on the XRD patterns was carried out in the diffraction angle range of 44.4–46°, and the results were displayed in Fig. 1b. Results showed that the Cu ion and Nb ion could be dissolved in a BCZT solution.

The radius of Nb^{5+}(r = 0.64 Å, Coordination Number = 6) and Cu^{2+} (r = 0.73 Å, Coordination Number = 6) were slightly larger than that of Ti^{4+} (r = 0.605 Å, Coordination Number = 6) and Zr^{4+} (r = 0.72 Å, Coordination Number = 6) correspondingly [22]. It was a possibility for Cu^{2+} and Nb^{5+} (CN) occupying B site to substitute Ti^{4+} or Zr^{4+} resulting in a change for the lattice parameter. Comparing to pure BCZT ceramics, the diffraction peaks of the BCZT-10CN ceramics shifted slightly to lower angles, suggesting that the value of the lattice parameters increased. However, with further rising CN content (x = 0.02), the diffraction peaks began to shift to higher angles. A possible explanation was due to partial Cu^{2+} and Nb^{5+} ions began to occupy the ions with larger radius in A sites, which resulted in the decrease of lattice parameters with high CN content.

According to the different characteristics of the {200} peaks in the perovskite structure, we can easily identify the distinction between tetragonal and rhombohedral phases [19]. And all peaks could be indexed based on the standard X-ray pattern of the tetragonal $BaTiO_3$ (JCPDS#05-0626). The coexistence of tetragonal and rhombohedral phase at all samples confirmed the morphotropic phase boundary (MPB) nature of these compositions [7]. In Fig. 1b, the sample of x = 0 showed that {200} peaks split into (002) and (200) peaks unevenly and (200) peaks was higher in the range of 44.4–46°, implying that the tetragonal and rhombohedral phases coexisted and tetragonal phase was the main phase. With the increase of x, the samples with compositions x = 0.01–0.02 showed {200} peaks splitting uniformly, indicating that tetragonal and rhombohedral phases coexisted evenly. The results revealed obvious changes in diffraction peaks near 2θ = 45°, indicating that CuO/Nb_2O_5 substitution could induce a structural phase transition from tetragonal phase which was the main phase of pure BCZT ceramics to

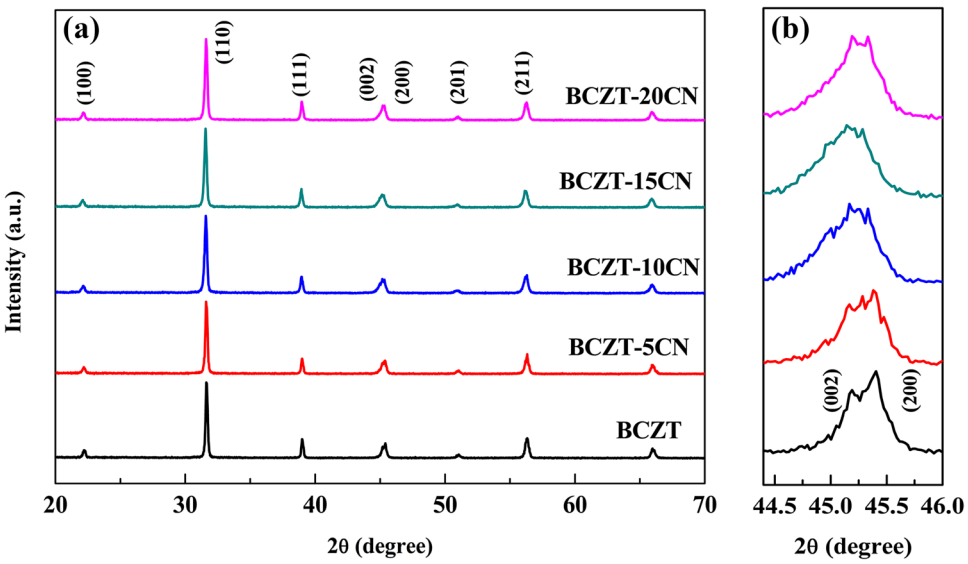

Fig. 1 **a** X-ray diffraction patterns of BCZT-1000xCN ceramics sintered at 1400 °C for 4 h. **b** The {200} peaks in the 2θ range of 44.4–46°

the mixture of rhombohedral and tetragonal phases equably with further increase of x.

Based on the XRD data 2θ range of 10–120° with slow scanning at 1 °/min, the variation of the lattice parameters (*a, b, c*) and the unit cell volume (V) for the BCZT-1000xCN ceramics were determined and shown in Fig. 2. Since the lattice parameters *a* was similar to *b*, the main crystal phase of ceramics was likely to be tetragonal phase and rhombohedral phases (T_{R-T} was reduced from 32 to 20 °C as discussed in Fig. 3). We could see that, with the increase of x, the variation of the lattice parameters (*a, b, c*) and the unit cell volume (V) were similar respectively. They increased initially, reached their maximum value at x = 0.01, and then decreased until x = 0.02. The slightly shift of diffraction peaks to lower angles was consistent with the increase in the lattice parameters and unit cell volume, which should be attributed to the bigger ionic radius of Cu and Nb in comparison with Ti. However, with further rising CN content (x = 0.015–0.02), the lattice parameters and unit cell volume began to decrease. A possible explanation was due to partial Cu^{2+} and Nb^{5+} ions began to occupy the ions with larger radius in A sites, which resulted in the decrease of lattice parameters and unit cell volume with large CN content. Moreover, the uniformly coexistence of tetragonal and rhombohedral phases was helpful to improve the electrical properties of ceramics at x = 0.01 [31]. The crystallographic data of refinement on the BCZT-1000xCN piezoelectric ceramics were given in Table 1.

As shown in Fig. 3, stripes and herringbone paterns could be observed in the similar grain. Obviously, the samples had different width of domain with different contents of CN. Figure 3 showed the temperature dependence of the dielectric properties for the BCZT-1000xCN ceramics, measured at 1 kHz. As can be seen, two obvious peaks were observed on the dielectric constant versus temperature curves in the measured temperature range between − 25 and 125 °C. It

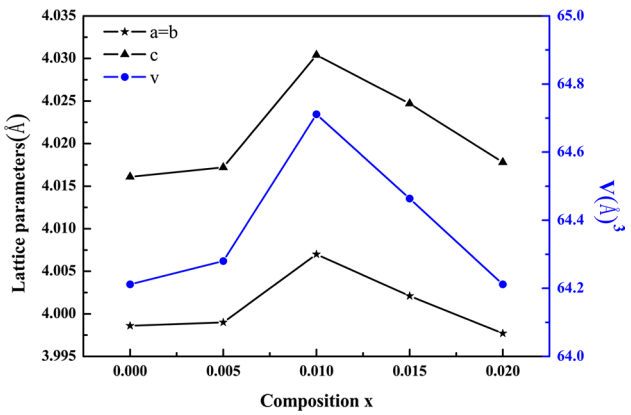

Fig. 2 Lattice parameters (*a, b, c*) and unit cell volume V for the BCZT-1000xCN ceramics

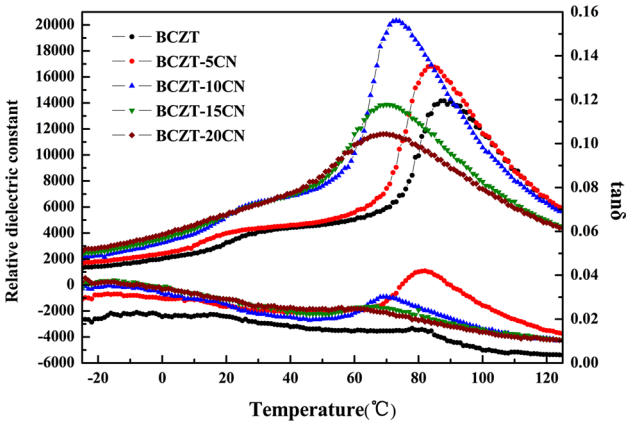

Fig. 3 Temperature dependence of the dielectric properties at 1 kHz for the BCZT-1000xCN ceramics sintered at 1400 °C for 4 h

was considered that these two peaks corresponded to the polymorphic phase transition from rhombohedral phase to tetragonal phase (T_{R-T}) and from tetragonal phase to cubic phase (T_C), respectively [18, 32]. The transition temperatures of T_{R-T} and T_C were about 30 and 85 °C, respectively. With increasing CN content, the T_C decreased from 88 to 75 °C.The variation tendency of T_{R-T} was similar to the T_C (from 32 to 20 °C). Comparing to pure BCZT ceramics, the characteristic peak of T_{R-T} and T_C shifted slightly to the low temperature, suggesting that the location of the Ti and Zr were replaced and led to lattice distortion with increasing CN content potentially. The decrease in T_C value reflected the incorporation of Cu^{2+} and Nb^{5+} into the BCZT lattice, and the amount of CN incorporated as solid solution also increased with the increasing of CN content. At the same time, the tricritical point of BCZT ceramics decreased, and could be shifted to room temperature with the increasing of CN content, as shown in the insert of Fig. 3. Achieving a polymorphic phase transition point at room temperature could improve the piezoelectric properties of $BaTiO_3$-based ceramics [18].

Figure 4a depicted the polarization–electric field (P–E) hysteresis loops of the BCZT-xCN ceramics as a function of x from 0.000 to 0.02 which were measured at 1 kHz under

Table 1 Crystallographic data of refinement on the BCZT-1000xCN ceramics

x	a (Å)	b (Å)	c (Å)	Unit-cell volume (Å^3)	Rwp (%)
0.00	3.9986	3.9986	4.0161	64.21	13.196
0.005	3.9990	3.9990	4.0172	64.28	12.955
0.01	4.0070	4.0070	4.0304	64.71	12.986
0.015	4.0021	4.0021	4.0247	64.46	13.263
0.02	3.9977	3.9977	4.0178	64.21	12.969

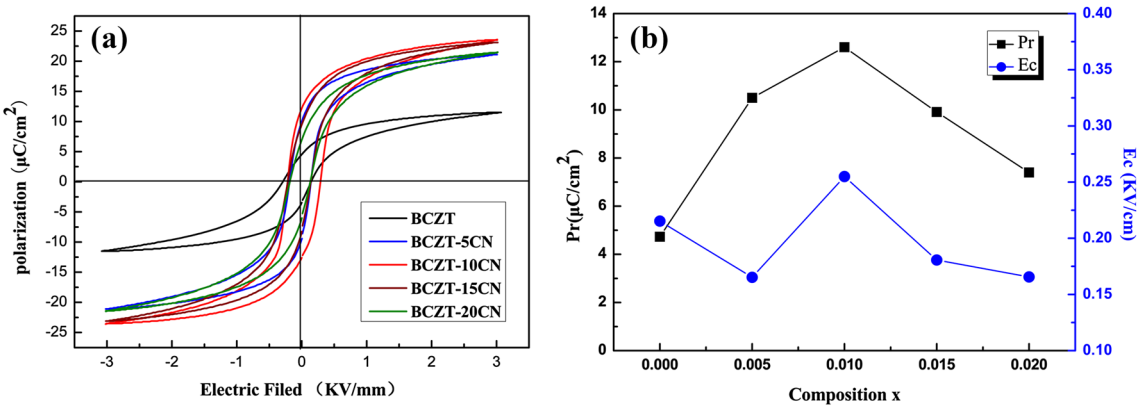

Fig. 4 **a** The polarization–electric field (P–E) hysteresis loops, **b** the remnant polarization (P_r) and coercive field (E_c) of the BCZT-1000xCN ceramics as a function of x from 0.00 to 0.02

an electrical field of 3 kV/mm near room temperature. All samples exhibited unsaturated and slim P–E loops with very low E_c, indicating that these materials were very "soft". The varying remnant polarization (P_r) and coercive field (E_c) were shown in Fig. 4b. It could be seen that the pure BCZT ceramics exhibited a worse ferroelectric polarization hysteresis loop, and the P–E loops became ameliorative with increased x. E_c decreased initially until x = 0.005–0.165 kV/cm, then raised sharply at x = 0.01–0.255 kV/cm, and subsequently droped. Besides, P_r increased initially, reaching the maximum value at x = 0.01–12.6 μC/cm^2, and then decreased until x = 0.02–7.4 μC/cm^2. The results of the coercive field (E_c) showed that the CN doped BCZT ceramics became softer and the ferroelectric properties strongly depended on Cu^{2+} and Nb^{5+} content. Distinctly, the sample with x = 0.01 had the largest P_r, suggesting that the increase oxygen vacancies would pin the domain to switch. It was well known that high P_r and low E_c might be ascribed to the coexistence of orthorhombic and tetragonal phases. Generally speaking, large remnant polarization usually facilitated the piezoelectric properties of the ceramics [32].

Figure 5 showed the variation of the piezoelectric strain constant (d_{33}) of pure $(Ba_{0.85}Ca_{0.15})(Zr_{0.10}Ti_{0.90})O_3$ under the condition of the poling time of 25 min with different polarization temperature and electric field. We chose 30 and 60 °C to explore polarization temperature because of the BCZT Curie temperature was around 90 °C. As illustrated in Fig. 5, with increasing the poling electric field of 2.5–5.0 kV/mm, the piezoelectric strain constant (d_{33}) increased gradually and both the 30 and 60 °C reached the maximum values of 349 and 335 pC/N, respectively. Besides, the piezoelectric properties of polarization temperature at 30 °C was better than 60 °C. The reason of this phenomenon might that the temperature of 60 °C was closer to the BCZT Curie temperature. When the ceramic was poled, the domain was easy to change direction and the polarization was more sufficient.

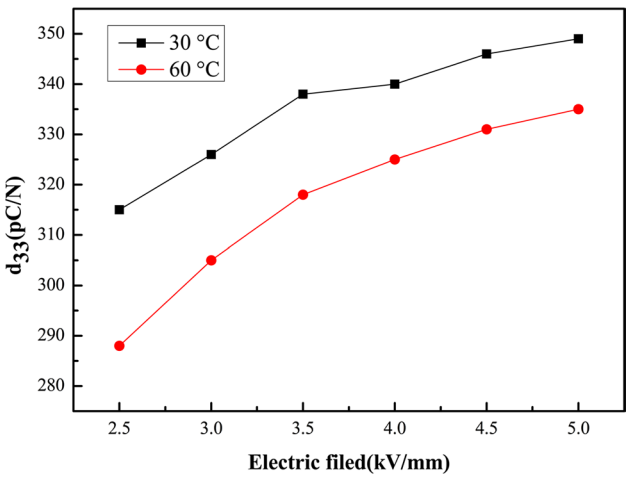

Fig. 5 Variation of the piezoelectric strain constant(d_{33}) of $(Ba_{0.85}Ca_{0.15})(Zr_{0.10}Ti_{0.90})O_3$ with the electric field at different polarization temperature

After removed the electric field, the temperature of the sample in the 60 °C started to reduce, and no applied voltage kept the direction of the electric domain. It resulted in some of the domains returning to the original direction. However, for the polarization sample near room temperature (30 °C), the domain activity was low and the electric domain was difficult to turn direction again after removed the electric field. Moreover, the volume fractions of domains might be much easier to be switched during poling for the ceramic with the coexistence of two phases when the poling temperature value was close to MPB [33]. Its d_{33} value gradually increased with the further increasing of E. It was believed that the higher poling electric field could be beneficial to the switching of domains in BCZT ceramics. But excessive poling electric field could cause samples breakdown and deteriorate piezoelectric properties in BCZT ceramics.

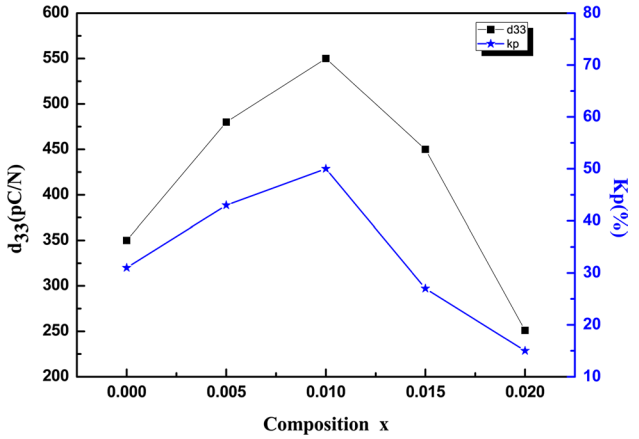

Fig. 6 Piezoelectric coefficient,d_{33} and planar mode electromechanical coupling coefficient, k_p values of the BCZT-1000xCN ceramics sintered at 1400 °C for 4 h

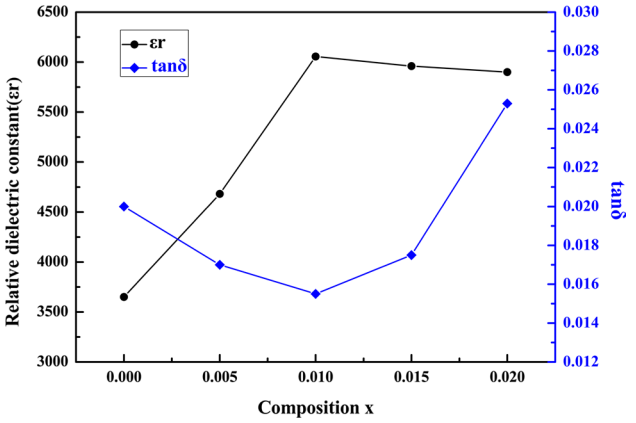

Fig. 7 Relative dielectric constant, ε_r and dielectric loss, tanδ of the BCZT-1000xCN ceramics measured at 1 kHz

Figure 6 showed the piezoelectric coefficient and planar mode electromechanical coupling coefficient of BCZT-1000xCN ceramics as a function of CN content. It could be observed that both d_{33} and K_p curves possessed a peak with the increased of CN content. With the raising of x to 0.01, both d_{33} and K_p reached their maximum value of 550 pC/N and 50%, respectively. It was believed that the observed high piezoelectric properties should be ascribed to the phase coexistence [18, 33–35] and the first-order phase transition occurring near room temperature should be the origin of this phase coexistence. It was well known that the radius of Cu^{2+} and Nb^{5+} were slightly larger than that of Ti^{4+}. Therefore, it was a possibility for Nb^{5+} and Cu^{2+} occupying B site to substitute Ti^{4+} resulted in the bigger lattice distortion, harder electric domain rotation and less orientation of electric domain along the direction of the electric field when CN doped amount increased. Therefore, it was possible that the piezoelectric properties decreased with the CN doped amount overmuch. Moreover, the high piezoelectric constant d_{33} phenomenon could be linked thermodynamically through the relation of $d_{33} = 2Q_{11}P_r\varepsilon^T_{33}$ [33], where Q_{11},P_r and ε^T_{33} respectively represented the electrostrictive coefficient, remnant polarization and dielectric constant. With the raising of x to 0.01, both the P_r and ε^T_{33} reached their maximum value of $P_r = 12.6\ \mu C/cm^2$ and $\varepsilon^T_{33} = 6056$ shown through Figs. 7 and 8b, separately.

In order to study the effect of CN addition on the dielectric behavior of BCZT ceramics, the relative dielectric constant ε_r and dielectric loss tanδ for BCZT-1000xCN ceramics measured at 1 kHz were shown in Fig. 7. As illustrated in Fig. 7, with increased x the relative dielectric constant ε_r (1 kHz) increased firstly for x up to 0.01 ($\varepsilon_{rmax} = 6056$) and then decreased with further x composition. However, the loss tangent (1 kHz) distinctly decreased at first and reached a minimum value of 1.55% at x = 0.01 CN addition. There was consensus among most experts that the BCZT ceramic defect reduced, energy consumption of domain wall motion decreased and dielectric loss decreased due to the increased density. When a small number of defects caused by doping the minor elements CN exists, it promoted the sintering process and increased the density of the BCZT ceramic. Therefore, the energy consumption of the domain wall motion was reduced. Because of these reasons, the relative dielectric constant decreased and dielectric loss increased. When CN doped amount was overmuch, Cu^{2+} and Nb^{5+} would not be completely dissolved in BCZT ceramics. There were a part of lattice distortion and impurity phase produced and deposited at grain boundaries, which resulted in the dielectric loss increasing. Therefore, the materials excessively doped with CN were easy to appear ion conductance loss phenomenon and would make the relative dielectric constant decrease and dielectric loss increase. Moreover, this component also had the minimum tanδ value of 1.55% owing to the denser microstructure (as listed in Fig. 8f) induced by the addition of CN [36]. The low tanδ and high ε_r indicated that the BCZT-1000xCN ceramics were promising applications for lead-free piezoelectric ceramics.

Figure 8a–e showed the surface morphologies of BCZT-1000xCN ceramics sintered at 1400 °C for 4 h. All samples showed high density with low porosity and the grain size decreased sharply and became uniform. When a small amount of CN was added, a dense microstructure with shrunken grains was developed (seen as Fig. 8a–e). Meanwhile, the uniformity of grains seemed to be improved by the increase addition of CN. The result was evident that CN addition caused a change on the grain size and dense microstructure, indicating that a small amount of liquid phases contributed to control the mobility of grain boundary to a certain degree so that a relative uniformity of grain was obtained and lowered the

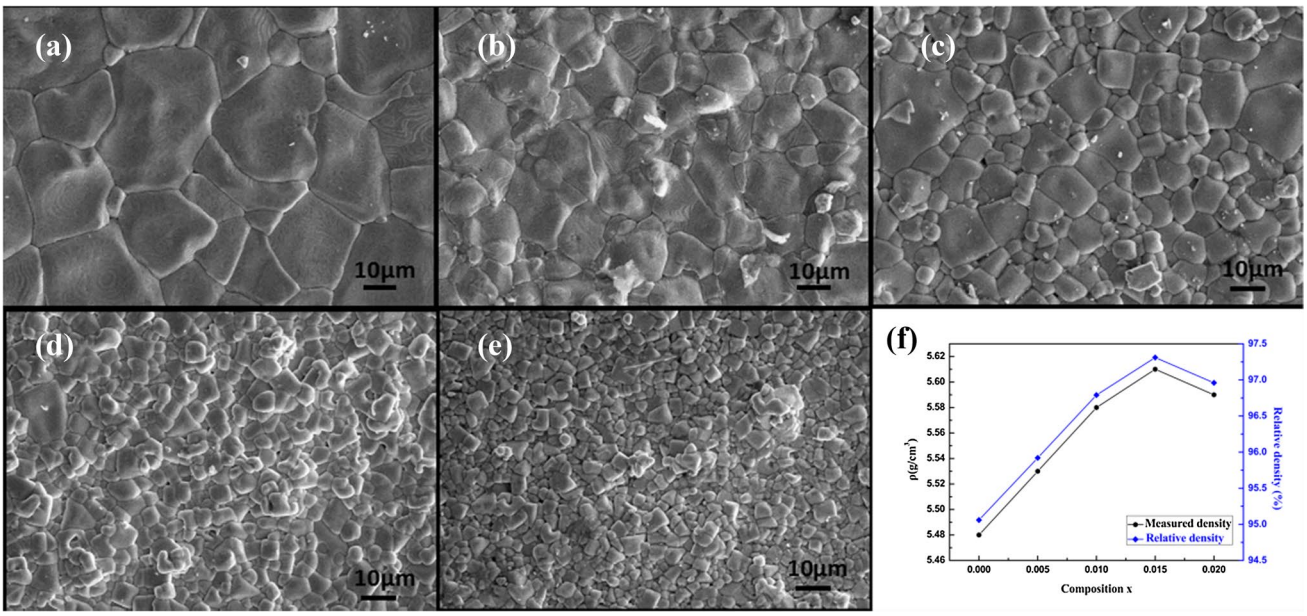

Fig. 8 SEM micrographs of BCZT-1000xCN ceramics: **a** x = 0.00; **b** x = 0.005; **c** x = 0.01; **d** x = 0.015; **e** x = 0.02; and **f** the measured density and relative density of BCZT-1000xCN ceramics

sintering temperature of BCZT ceramics [37, 38]. The measured density with Archimedes method and relative density of CN codoped specimens were shown in Fig. 8f. It could be seen that the measured density and the relative density increased firstly, and then decreased with further increasing CN amount. Both the measured and relative densities reached the maximum values of 5.61 g/cm^3 and 97.31% at x = 0.015, respectively. The variations trend of SEM and density could be attributed to the low melting points of CuO (1026 °C) additives. And the lower sintering temperature of BCZT here could be partly attributed to the formation of CuO-BaO transient liquid phase (eutectic point ~ 925 °C) during the earlier sintering process. These consequences promoted the grain uniform and the densification behavior by facilitating the dissolution and migration of the species [14, 39]. In the later stage, Cu^{2+} and Nb^{5+} ions would enter into the ceramics lattice to substitute the ions at A or B sites and improve the properties of ceramics. However, when the doping content further increased, the liquid phase would be separated out and form glass phase, which would deteriorate overall performance of samples. Moreover, the surface micrographs of BCZT-1000xCN (x = 0.02) ceramics were similarity to the pure BCZT ceramics, indicating that Cu-rich liquid phase(s) segregated at the grains boundaries when the CN content was higher than its solid solubility limited in crystal structure in the ceramics with further increasing x above 0.015. A larger amount of the intergranular liquid phase(s) might result in voids and inhibit both densification and uniform grain of the ceramics [40, 41]. Therefore, it was believed that the proper amount of CN addition to BCZT ceramics could make the grain refinement and result in a reduction of sintering temperature.

Figure 9 depicted the particle size distribution of the BCZT-1000xCN ceramics sintered at 1400 °C for 4 h with different x. It could be seen that with the raising of x, the mean particle size decreased gradually from x = 0.00–25.9 μm to x = 0.02–3.2 μm and the standard deviation decreased gradually from x = 0.00–9.4 to x = 0.02–1.2. It indicated that the grain size was decreased and the uniformity of grain was improved by the increased addition of CN. Among the various reasons for this phenomenon, high density of crystal nucleus at the early stage of sintering by adding CN played the most important role. It reduced the collision distance among nucleation sites during early phase transformation and restricted the dendritic crystal growth in sintering process. As a consequence, a uniform and fine crystallized microstructure was formed. Meanwhile, the CuO-BaO transient liquid phase was formed during the earlier sintering process. It indicated that a small amount of liquid phases contributed to control the mobility of grain boundary to a certain degree so that a relative uniformity of grain was obtained. Furthermore, the radius of Cu^{2+} and Nb^{5+} were close to BCZT ceramics. Thus, it was easy to form a solid solution phase with the main crystal phase and then caused lattice distortion. In this case, the number of defects increased and the particles were easier to move, so that the sintering was accelerated. However, when the doping content overmuch, the liquid phase would be separated out and formed glass phase overabundance, which would

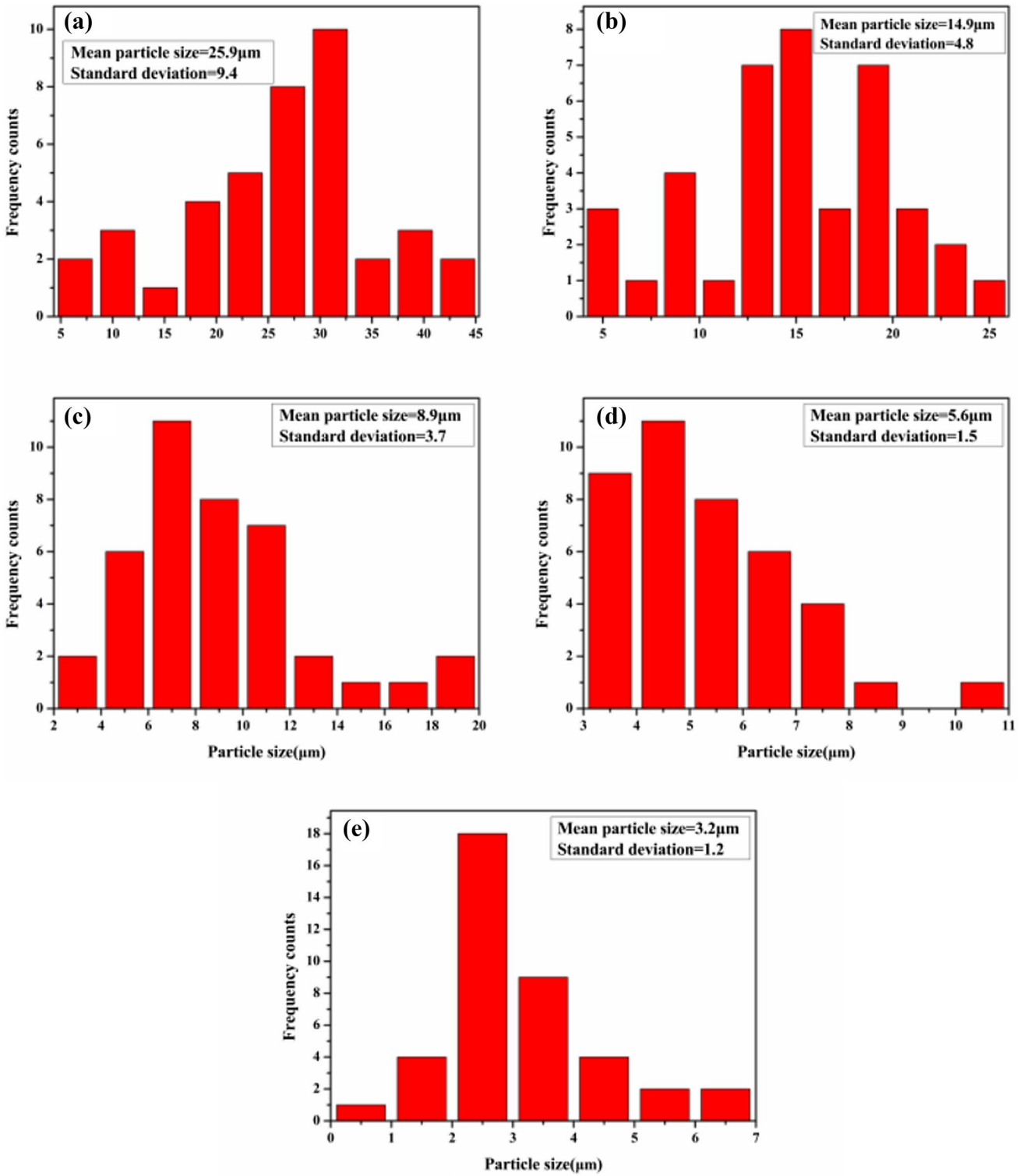

Fig. 9 The particle size distribution of the BCZT-1000xCN ceramics sintered at 1400 °C for 4 h: **a** x = 0.00; **b** x = 0.005; **c** x = 0.01; **d** x = 0.015; **e** x = 0.02

deteriorate piezoelectric properties of samples. Therefore, it was believed that the proper amount of CN addition and the suitable particle size could improve the piezoelectric properties of BCZT-1000CN ceramics(as discussed in Fig. 6).

4 Conclusions

Lead-free $(Ba_{0.85}Ca_{0.15})(Zr_{0.10}Ti_{0.90})_{1-x}(Cu_{1/3}Nb_{2/3})_xO_3$ piezoelectric ceramics were prepared by the conventional solid-state reaction sintering process in air, and it was found that the polymorphic phase transition point of the ceramics were shifted to room temperature by the introduction of CuO/Nb_2O_5. The crystalline phases,dielectric and piezoelectric properties of the ceramics were studied. X-ray diffraction(XRD) data showed that the ceramics containing CuO/Nb_2O_5 still showed the coexistence of tetragonal and rhombohedral phases similar to the undoped samples. The study found that adding a small amount of CuO/Nb_2O_5 into BCZT ceramics could largely reduce the sintering temperature. Main piezoelectric parameters were optimized nearly at $x = 0.01$ with $d_{33} = 550$ pC/N, $k_p = 50\%$ and $P_r = 12.6$ μC/cm^2, owing to the room-temperature about 20 °C the polymorphic phase transition point induced by doping with CN. Besides, the BCZT-10CN ceramic demonstrated an enhanced dielectric properties ($\varepsilon_{rmax} = 6056$ and $\tan\delta = 1.55\%$) at room temperature and a relevant low sintered temperature of 1400 °C, showing a promising candidate for the transducer and transformer applications.

References

1. A.S. Karapuzha, N.K. James, S.V.D. Zwaag, W.A. Groen, J. Mater. Sci. Mater. Electron. **27**, 1–7 (2016)
2. J. Rödel, W. Jo, K.T.P. Seifert, E.M. Anton, T. Granzow, D. Damjanovic, J. Am. Ceram. Soc. **92**, 1153–1177 (2009)
3. E.M. Sabolsky, L. Maldonado, M.M. Seabaugh, S.L. Swartz, J. Electroceram. **25**, 77–84 (2010)
4. Y. Saito, H. Takao, T. Tani, T. Nonoyama, K. Takatori, T. Homma, T. Nagaya, M. Nakamura, J. Nat. **432**, 84–84 (2004)
5. Y. Zhang, B. Liu, B. Shen, J. Zhai, J. Mater. Sci. Mater. Electron. **28**, 11114–11118 (2017)
6. K. Xu, J. Li, X. Lv, J.G. Wu, X.X. Zhang, D.Q. Xiao, J.G. Zhu, J. Adv. Mater. **28**, 8519–8523 (2016)
7. Z.Z. Zhao, X.L. Li, H.H. Ji, Y.J. Dai, T. Li, J. Alloy. Compd. **637**, 291–296 (2015)
8. D.Q. Xiao, J.G. Wu, L. Wu, J.G. Zhu, P. Yu, D.M. Lin, Y.W. Liao, Y. Sun, J. Mater. Sci. **44**, 5408–5419 (2009)
9. J.G. Wu, Y.Y. Wang, D.Q. Xiao, J.G. Zhu, J. Appl. Phys. Lett. **91**, 132914–132917 (2007)
10. J.G. Wu, D.Q. Xiao, W.J. Wu, Q. Chen, J.Q. Zhu, Z.C. Yang, J. Wang, J. Scripta Mater. **65**, 771–774 (2011)
11. X.P. Wang, J.G. Wu, X. Lv, H. Tao, X.J. Cheng, T. Zheng, B.Y. Zhang, D.Q. Xiao, J.Q. Zhu, J. Mater. Sci. Mater. Electron. **25**, 3219–3225 (2014)
12. J.G. Wu, Z. Fan, D.Q. Xiao, J.G. Zhu, J. Wang, J. Prog. Mater. Sci **84**, 335–402 (2016)
13. X.P. Wang, J.G. Wu, D.Q. Xiao, J.G. Zhu, X.J. Cheng, T. Zheng, B.Y. Zhang, X.J. Lou, X.J. Wang, J. Am. Chem. Soc. **136**, 2905–2910 (2014)
14. Y.J. Dai, S.S. He, X. Lao, S.Z. Zhang, J. Am. Ceram. Soc. **97**, 1283–1287 (2014)
15. X.J. Cheng, J.G. Wu, X.J. Lou, X.J. Wang, X.P. Wang, D.Q. Xiao, J.G. Zhu, J. ACS Appl. Mater. Interfaces **6**, 750–756 (2014)
16. N. Vittayakorn, C. Puchmark, G. Rujijanagul, X. Tan, D.P. Cann, J.Curr. Appl. Phys **6**, 303–306 (2006)
17. R. Bechmann, J. Acoust. Soc. Am. **28**, 347–350 (1956)
18. W.F. Liu, X.B. Ren, J. Phys. Rev. Lett. **103**, 257602 (2009)
19. D.S. Yin, Z.H. Zhao, Y.J. Dai, Z. Zhao, X.W. Zhang, S.H. Wang, J. Am. Ceram. Soc. **99**, 2354–2360 (2016)
20. J.G. Hao, W.F. Bai, W. Li, J.W. Zhai, J. Am. Ceram. Soc. **95**, 1998–2006 (2012)
21. H.X. Bao, C. Zhou, D.Z. Xue, J.H. Gao, X.B. Ren, J. Phys. D. Appl. Phys. **43**, 465401–465404 (2010)
22. J. Wu, D. Xiao, W. Wu, J. Zhu, J. Wang, J. Alloy. Compd. **509**, L359-L361 (2011)
23. I. Burn, P. US Patent 4283753 (1981)
24. H.Y. Tian, K.W. Kwok, H.L.W. Chan, J. Mater. Sci. **42**, 9750–9755 (2007)
25. D.Y. Liang, X.H. Zhu, J.L. Zhu, J.G. Zhu, D.Q. Xiao, J. Ceram. Int. **40**, 2585–2592 (2014)
26. C.F. Yang, L. Wu, T.S. Wu, J. Mat. Sci. **27**, 6573–6578 (1992)
27. P. Zheng, J.L. Zhang, S.F. Shao, Y.Q. Tan, C.L. Wang, J. Appl. Phys. Lett. **94**, 032902–032904 (2009)
28. P. Parjansri, U. Intatha, S. Eitssayeam., J. Mater. Res. Bull. **65**, 61–67 (2015)
29. Y. Cui, X. Liu, M. Jiang, Y. Hu, Q. Su, H. Wang, J. Mater. Sci. Mater. Electron. **23**, 1342–1345 (2012)
30. X. Wang, P. Liang, L. Wei, X. Chao, Z. Yang, J. Mater. Sci. Mater. Electron. **27**, 1–10 (2015)
31. J.G. Wu, D.Q. Xiao, J.G. Zhu, J. Chem. Rev. **115**, 2559–2595 (2015)
32. X.F. Wang, P.F. Liang, X.L. Chao, Z.P. Yang, J. Ceram. Int. **40**, 9389–9394 (2014)
33. J.G. Wu, D.Q. Xiao, W.J. Wu, Q. Chen, J.G. Zhu, Z.C. Yang, J. Wang, J. Eur. Ceram. Soc. **32**, 891–898 (2012)
34. P. Wang, Y.X. Li, Y.Q. Lu, J. Eur. Ceram. Soc. **31**, 2005–2012 (2011)
35. M.J. Haun, E. Furman, Z.Q. Zhuang, S.J. Jang, L.E. Cross, Ferroelectrics **94**, 313–313 (1989)
36. Y.C. Lee, Y.L. Huang, J. Am. Ceram. Soc. **92**, 2661–2667 (2009)
37. C.C. Tsai, S.Y. Chu, C.H. Lu, J. IEEE. Trans. Ultrason. Ferroelectr. Freq. Control **56**, 660 (2009)
38. D. Hou, M.K. Zhu, H. Wang, B. Wang, H. Yan, C.S. Tian, J. Mater. Sci. Eng. B **110**, 27–31 (2004)
39. L. Zhao, B.P. Zhang, P.F. Zhou, X.K. Zhao, L.F. Zhu, J. Am.Ceram. Soc. **97**, 2164–2169 (2014)
40. H.J. Sun, Y. Zhang, X.F. Liu, Y. Liu, W. Chen, J. Ceram. Int. **41**, 555–565 (2015)
41. Y. Cui, X.Y. Liu, M.H. Jiang, J. Mater. Sci. Mater. Electron. **23**, 1342–1345 (2012)